Modeling and Analysis

Biofpr Biofuels Bioproducts & Biorefining

Determining optimal size reduction and densification for biomass feedstock using the BioFeed optimization model

Yogendra N. Shastri,* Zewei Miao, Luis F. Rodríguez, Tony E. Grift, Alan C. Hansen, and K.C. Ting, Energy Biosciences Institute & Department of Agricultural and Biological Engineering, Urbana, IL, USA

Received June 25, 2013; revised January 10, 2014, and accepted January 13, 2014
View online at Wiley Online Library (wileyonlinelibrary.com); DOI: 10.1002/bbb.1476;
Biofuels, Bioprod. Bioref. **(2014)**

Abstract: The benefits of particle size reduction and mechanical densification of biomass feedstock for storage, transportation, and handling must be assessed in relation to the systemic costs and energy consumption incurred due to these operations. The goal of this work was to determine the optimal levels of size reduction and densification through a combination of modeling and experimental studies. Size reduction and densification data for Miscanthus and switchgrass were generated using a two-stage grinding process and the energy requirement and bulk densities for the particle sizes between 1 mm and 25.4 mm were determined. Increase in bulk density through compression by a pressure of 1.2 MPa was also measured. These data were used within BioFeed, a system-level optimization model, to simulate scenarios capturing the possibilities of performing size reduction and densification at various stages of the supply chain. Simulation results assuming size reduction at farms showed that the optimal particle size range for both Miscanthus and switchgrass was 4–6 mm, with the optimal costs of \$54.65 Mg^{-1} and \$60.77 Mg^{-1} for Miscanthus and switchgrass, respectively. Higher hammer mill throughput and lower storage costs strongly impacted the total costs for different particle sizes. Size reduction and densification of biomass at the county-specific centralized storage and pre-processing facilities could reduce the costs by as much as \$6.34 Mg^{-1} for Miscanthus and \$20.13 Mg^{-1} for switchgrass over the base case. These differences provided the upper bound on the investments that could be made to set-up and operate such systems. © 2014 Society of Chemical Industry and John Wiley & Sons, Ltd

Supporting information may be found in the online version of this article.

Keywords: biomass feedstock; size reduction; densification; BioFeed; hammer milling; Miscanthus; switchgrass

Correspondence to: Yogendra N. Shastri, Room 311, Department of Chemical Engineering, Indian Institute of Technology Bombay, Powai, Mumbai – 400076, India. E-mail: yshastri@iitb.ac.in
*This research was carried out when this author was a Visiting Research Assistant Professor at Energy Biosciences Institute, University of Illinois at Urbana-Champaign.

SCI

Introduction

Cost-effective and efficient production and provision of biomass feedstock is essential for the success of the second-generation biofuel sector. It is expected that agricultural feedstocks such as dedicated energy grasses and agricultural residue will play an important role in meeting the targeted goals.[1,2] However, the production and provision of these feedstocks such as Miscanthus, switchgrass, corn stover, and sweet sorghum are highly inefficient due to their low energy and bulk densities.[3] These low densities lead to large storage, transportation, and handling requirements, thereby adding to the overall cost of the feedstock at the refinery gate. Size reduction and densification of biomass feedstock can overcome these challenges to a certain extent.[4,5] Chopping or grinding to smaller particle sizes has been shown to increase the bulk densities,[6] and densification will further increase the density. Size reduction is also beneficial for biomass processing as a smaller particle size leads to enhanced conversion efficiency, possibly due to greater surface area.[7] However, the costs and energy consumption of size reduction and densification can be substantial, and those costs must also be considered in conjunction with the benefits in order to make the appropriate decisions. This calls for a systems-based approach.

In this work, we have used the BioFeed optimization model to perform this analysis.[8,9] BioFeed is a system-level model that incorporates important feedstock production and provision activities and determines the optimal system design and management strategies. This work used BioFeed to study the systemic impacts of size reduction and densification on Miscanthus and switchgrass production systems. Lack of reliable experimental data had hindered such an analysis in the past. We have, therefore, also conducted size reduction and densification experiments to generate the required data to use within the BioFeed modeling framework. This study, therefore, represents a unique integration of modeling and experimentation to explore the complexities of the feedstock production systems. The objective was to quantify the trade-offs associated with size reduction and densification, to determine their optimal levels, and to provide recommendations to further improve the system performance.

The paper is arranged as follows: The next section describes the details of the size reduction and densification experiments conducted in this work, while the BioFeed model along with the scenarios modeled are presented in the subsequent section. The experimental and simulation results are then discussed, followed by the main conclusions and recommendations.

Size reduction and densification experiments

Miscanthus and switchgrass were established in 2008 at the Energy Farm of the University of Illinois at Urbana-Champaign (40.1096°N, 88.2042 °W). The biomass was harvested using a mower-conditioner and baled using a square baler in the early spring of 2009 and 2010.[6] Both crops were left standing in the field during winter before harvesting. Miscanthus and switchgrass bales were stored for one year in a roofed open-air storage building, and selected randomly for this study. Miscanthus bales consisted of approximately 70–80% stem material and 20–30% sheath and leaf material, whereas switchgrass bales consisted of 55–70% stem material and 30–45% sheath and leaf material. Moisture content of Miscanthus and switchgrass samples ranged from 7% *w/w to* 20% *w/w*.

Size reduction experiments

This work used data generated for the lab-scale size reduction experiments of Miscanthus and switchgrass, which were carried out following a two-stage mechanical chopping process, i.e. coarse and fine size reduction. A commercial scale David Bradley hammer mill was used (5152W, Westinghouse Electric Corporation, Sears Roebuck and Co., Hoffman Estates, IL, USA) to grind 3 kg of unbaled Miscanthus (approximately 0.3~1.2 m long) and switchgrass (about 0.16~0.6 m long) through the 6.35-mm or 12.7-mm circular-opening screens. This step was termed 'coarse size reduction'. The second step was to further reduce the coarse biomass particles into finer particles with a Retsch SM2000 knife mill. For the knife mill, the aperture sizes of the milling screen included 1-mm trapezoidal, and 2-, 4-, 6-, and 8-mm square openings.[6] Each treatment was repeated three times.

The energy consumption of the milling machine was measured using a Yokogawa CW120/121 clamp-on power meter (IM CW120-E, Yokogawa M&C Corporation, Newnan, GA, USA). To determine the magnitude of fluctuations in current over time caused by varying mechanical friction, idle power consumption was measured for each machine during four repetitions. A 95% confidence level with a normal distribution was used to determine whether the power consumption surge resulted from milling biomass materials or from current fluctuation caused by mechanical friction. The real-time throughputs of the milling machines were recorded using a scale and LP7510 weighing indicator (Indiana Scale Company Inc., Terre Haute, IN, USA). Bulk densities of the ground biomass

were measured following the ASAE standard S269.4 DEC 1991 (R2007).[10] Each measurement was repeated three times and the variation in bulk density and specific energy of size reduction with the particle size was determined. It is important to note that the different particle sizes considered here are in fact the aperture size of the screen of the milling machine, and data such as bulk density for a specific particle size pertain to the biomass ground through that particular screen.

Densification experiments

Biomass densification experiments were performed at the mini-bale scale (Fig. 1).[11] The dimensions of the mini-bale chamber, custom built in our laboratory at the University of Illinois, were 0.15 × 0.15 × 0.203 m (0.00456 m^3). The container was filled with up to 0.4–0.5 kg samples. Subsequently, the material was compressed to a pressure of 5.5 MPa, which translated into 1.2 MPa pressure applied to the biomass. This pressure level was approximately 1.5 times the working pressure (0.5~1 MPa) of a New Holland large square baler.[12] A hydraulic compressor was built to measure specific energy consumption of biomass densification. A MATLAB® program was developed and used to combine data acquisition and analysis. This program measured the displacement of the piston and the hydraulic cylinder pressure at a rate of 100 samples per second using a low-cost USB data acquisition module (NI 6009, National Instruments Austin, TX, USA). After completion of the test, the same MATLAB® program fitted pressure-displacement curves and calculated the densification energy consumption during the test. This allowed the calculation of the variation in bulk density after densification and the specific energy of densification as a function of particle size. This work did not consider rebounding effects of biomass after removal of pressure.

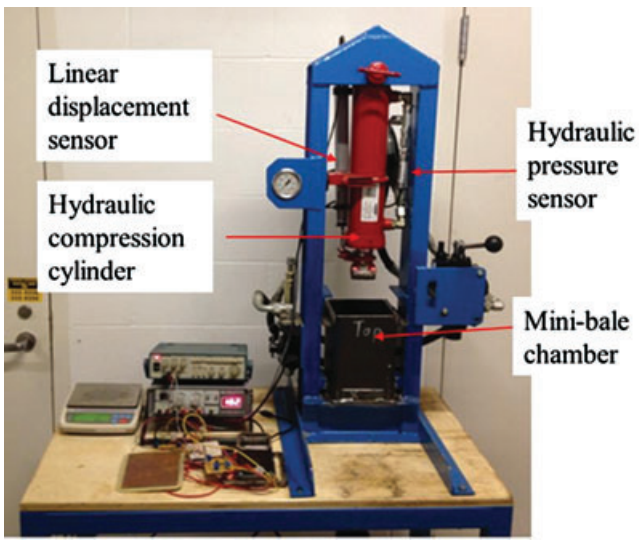

Figure 1. Densification apparatus consisting of a hydraulic cylinder and a mini-bale densification chamber.[11] The apparatus was instrumented to read the hydraulic cylinder pressure and displacement using an NI 6009 USB data acquisition unit. LabVIEW® was used for testing, while a MATLAB® program performed data acquisition and analysis during the experiments.

BioFeed model

The BioFeed model has been developed by this group at the Energy Biosciences Institute, University of Illinois at Urbana-Champaign. The main components of the BioFeed model are various feedstock production and provision operations before its delivery to the biorefinery (Fig. 2).[8,9,13] BioFeed models a scenario where many farms are producing biomass feedstock for one or more regional biorefineries, and models the important operations along this value chain. The model assumes that standard crop-establishment techniques will be used that will result in a mature, harvestable stand of biomass on each farm. For each farm under consideration, the production activities include harvesting, raking, post-harvest pre-processing, in-field transport, handling, on-farm storage, and ensilage. The packed biomass can either be directly transported to the biorefinery, or stored in one of the three storage options: on-farm open storage, on-farm covered storage, and centralized (satellite) storage. The satellite storage facilities are shared by multiple farms in the region and can include mechanical pre-processing of biomass, such as size reduction and densification.[14] The pre-processing can be performed at the input or the output of the storage facilities, which has an impact on the storage volume requirements. The transportation activities are carried out using a fleet of trucks that is independently owned. The impact of regional weather on the harvesting activities is modeled by incorporating the probability of working day (pwd) parameter in the model equations.[15]

Each compartment is modeled using a set of linear algebraic equations that reflect the mass balance as well as the equipment capacity and availability constraints. The decision variables include equipment selection and their operating schedules, biomass distribution among various alternatives, on-farm storage method selection and sizing, centralized storage selection and sizing, transportation fleet size selection and utilization of the fleet (logistics), number of pre-processors at the satellite storage facilities

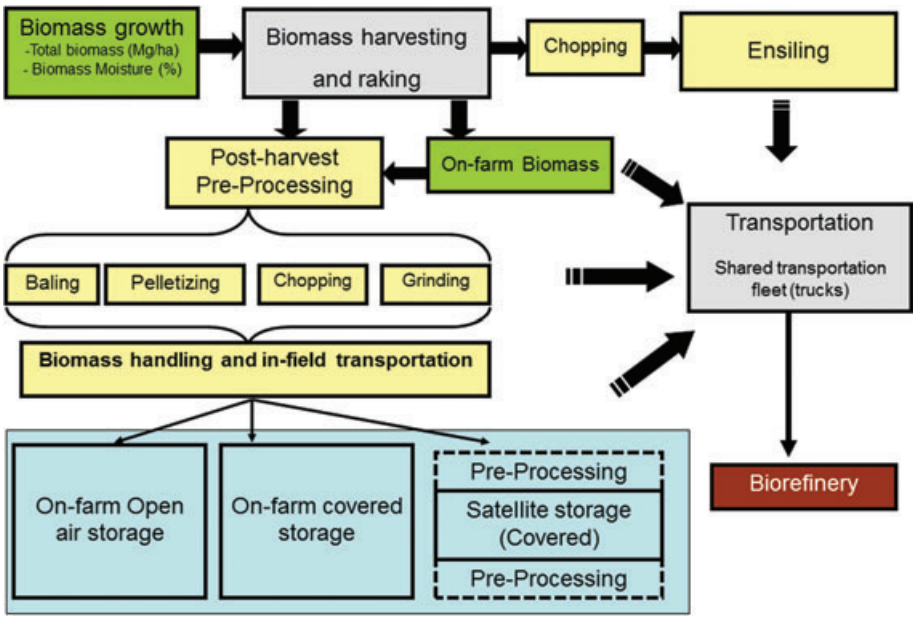

Figure 2. BioFeed model: Each compartment is modeled using a set of algebraic equations that constitute the constraints in the optimization model.[13]

if pre-processing is performed at those facilities, and the biorefinery capacity. All the decisions are simultaneously optimized for each farm as well as the rest of the production and provision system, resulting in a mixed integer linear programming (MILP) model. The simulation period consists of one year, which is divided into a harvesting and non-harvesting period. Biomass harvested during the harvesting period, which typically lasts for 2–4 months, must be stored and supplied to the biorefinery during both the harvesting and non-harvesting periods. The smallest simulation time step is one day, and the user can specify a larger time step consisting of multiple days. Although a smaller time step is desired for greater accuracy, reducing the time steps increases the solution time significantly.

Each operation is associated with fixed as well as operating costs. The operating costs include labor, fuel and lube, and repairs. The goal of the model is to optimize all decisions simultaneously so that the best system-level configuration can be determined. The objective function, therefore, is the maximization of the total system profit by assuming a fixed biorefinery gate price in \$ Mg^{-1}. The division of the total profit among various stakeholders is not considered. It is possible to specify the type and number of equipment *a priori* to build specific scenarios. The model has been developed in GAMS (General Algebraic Modeling System).[16] A novel computational scheme called DDC (Decomposition and Distributed Computing) is used to solve the MILP problem in a computationally efficient manner.[17] The individual MILP problems generated after the implementation of the DDC approach are solved using the CPLEX® solver. The total cost calculated by the model and reported later as part of results is the combined cost of all operations modeled by BioFeed. This includes harvesting, raking, storage, pre-processing, infield transportation, loading and unloading, and long-distance transportation. The farmland cost as well as crop establishment, fertilization, and irrigation costs are not considered.

Model scenario basics

The simulation studies in this work modeled Miscanthus and switchgrass production in southern Illinois. The scenarios for these two feedstocks were modeled independently to compare their relative costs, as we did not consider simultaneous production of the two feedstocks for a single biorefinery. The scenarios included a collection area of 17 400 km^2 distributed among 13 counties (map of the collection region shown in supporting information, Fig. S1). The actual energy crop farm area was about 670 km^2 divided over 284 farms. The farm sizes were based on the typical farm size distribution in Illinois.[18] A biorefinery was assumed to exist at Nashville, IL, and its capacity was optimized by the model. The transportation distances between farms, satellite storage facilities, and the biorefinery were calculated using Google Maps® (http://maps.google.com/). The peak dry matter yields of Miscanthus

and switchgrass on September 1 were 28 Mg ha^{-1} and 12 Mg ha^{-1}, respectively, and the biomass loss rates for non-harvested, standing crop of Miscanthus and switchgrass were 0.07 Mg d^{-1} ha^{-1} and 0.01 Mg d^{-1} ha^{-1}, respectively.[19] The harvesting season for Miscanthus was January to April (four months) during which time the harvestable yield dropped linearly from 20 Mg ha^{-1} to 11 Mg ha^{-1}. The harvesting season for switchgrass was between September and December (four months) during which the harvestable yield dropped linearly from 12 Mg ha^{-1} to 7.2 Mg ha^{-1}. We assumed that the moisture content for both crops at peak yield on September 1 was 60% and reduced linearly thereafter at the rate of 0.3% d^{-1} to a minimum moisture content of 15%. The short-term variations in the moisture content due to weather variability were ignored, but could be included in future model extensions. The equipment performance data for Miscanthus reported in European studies[20,21] in combination with the ASABE machinery standards[22,23] were used in this work. The equipment performance data for switchgrass production were based on Shastri *et al*.[8] and Kumar and Sokhansanj.[24] The data for typical farm equipment such as loaders, fork lifts, and trailers that were not crop-specific were adopted from Sokhansanj.[25] The biomass storage data were from Shastri *et al*.[9] The equipment data tables are provided in the supporting information (Tables S1–S12). The model assumed that on-farm open storage was on a gravel pad, and the satellite storage was in the form of an enclosed facility without ventilation. The type of on-farm covered storage depended on the pre-processing performed on the farm and is mentioned while discussing each scenario.

Size reduction scenarios: Base case

Various scenarios were studied to quantify the impact of size reduction and densification to different levels. The base case set of scenarios (Fig. 3) assumed that the pre-processing (size reduction) of biomass was carried out on-farm after harvesting and moving it to the edge of the farm. The ground biomass was then stored on-farm or at the satellite storage facilities, and this distribution was optimized by the BioFeed model. Only covered storage with three walls was considered for on-farm storage since open storage of ground biomass could lead to substantial losses due to weather events such as rain and high wind. The satellite storage facility was assumed to be located at Okawville, IL, which was about 20 km from the biorefinery. This led to an average distance of 70 km between the farms and the storage location, as well as between farms and the biorefinery. Eight scenarios, each individually

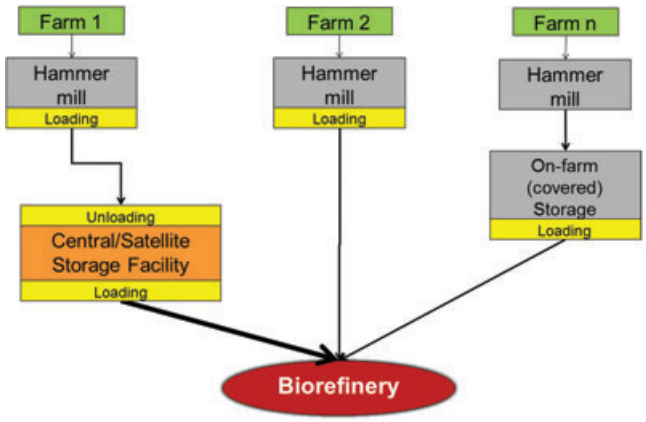

Figure 3. Base case size reduction scenario for BioFeed; on-farm size reduction was performed on each farm to specific particle sizes using a hammer mill; ground biomass was stored on-farm or transported to storage or biorefinery without any densification; ground biomass storage was optimized between on-farm covered storage and the satellite storage facility.

optimized, were simulated where the particle size was specified to 1, 2, 4, 6, 8, 12.7, 16, and 25.4 mm. In each scenario, each farm used a hammer mill to achieve the specified particle size. This ensured that the biorefinery received a uniform biomass form.

Size reduction and densification scenarios

The second set of scenarios considered size reduction as well as densification of biomass feedstock. Pelletization or briquetting are densification options that have been studied in the past. However, pellets and briquettes need to be disintegrated into ground or powdered form before processing. Cost of pelletization is also significant. Therefore, we explored temporary densification options during the transportation of biomass. Here, we envisioned a loading mechanism and a truck similar to the garbage pick-up truck that compresses material temporarily. The truck would generate enough pressure to achieve the necessary densification and maintain it during the transportation so that the volume and weight limits of the truck are achieved simultaneously. This will lead to optimal utilization of the individual truck. Compression pressure will be removed after transportation, and biomass will return close to its original bulk density. Such densification can be modeled during all stage of transportation. However, densification during transportation between farms and biorefinery or storage facilities would require the specialized equipment to

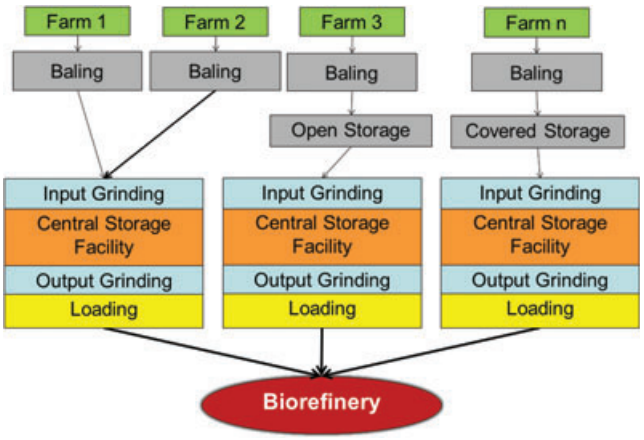

Figure 4. Size reduction and densification scenarios modeled using BioFeed; size reduction was performed at the input or output of the centralized storage and pre-processing (CSP) facilities in each county and ground biomass could be compressed during transportation by using special loading and transport equipment.

be set-up on every farm and the custom designed trucks to be used extensively. This is not expected to be cost-effective. Instead, the installation of such equipment at the satellite storage facilities would be a more cost-effective option.[5,26] Therefore, we modeled a size reduction and densification scenario where the supply system consisted of centralized storage and pre-processing (CSP) facilities in each county (Fig. 4).[14] Farmers baled the energy crops and transported those to the CSP of that county. This reduced the average distance between farms and the storage locations to about 19 km, while the average distance between the storage locations and the biorefinery was about 67 km. On-farm storage of bales could be open on gravel pad or covered with a shed without any walls. At the CSPs, size reduction could be performed either at the input before storage or at the output before transportation to the biorefinery, and the storage requirements changed accordingly. Size reduction at both input and output was not modeled. Storage at CSPs was without densification. Ground biomass could be transported to the biorefinery in uncompressed as well as compressed form. Thus, four scenarios with combination of two locations of size reduction at CSPs and option of densification during transportation were modeled. The compression pressure was assumed to be 1.2 MPa so as to use the experimental results previously presented. The advantage of such an arrangement was that regular flat-bed trailers could be used for transportation between farms and CSPs. Specialized loading and transport equipment would be needed only for transport between CSPs and biorefinery. Since the total amount of biomass handled at each CSPs would be much higher than at individual farms, the resulting economy of scale was expected make such installations cost-effective.

It must be emphasized that the optimization problem did not consider the cost of densification. Therefore, the results presented later, subject to this assumption, must be interpreted carefully. This is discussed later while describing the results.

It is also important to note that according to valid volume (width × height × length: 2.3×2.7×12.2 m~16.2 m) of the widely-used commercial transport vehicles in North America and legal load standard (19.7 Mg per truck) of the US Department of Transportation for highway, the upper-limit of biomass bulk density is about 220–250 kg m^{-3} for road transportation with a flatbed trailer or wagon. The bale bulk density of 220–250 kg m^{-3} has been achieved in-field with a regular baling machine and average baling speed by chopping the biomass into 15–20-cm long pieces at the Energy Farm of University of Illinois at Urbana-Champaign. The data used for model simulations matched these guidelines. The BioFeed model accounts for volume as well as weight constraints of the transportation equipment while determining the number of trucks.

The scenarios considered here may also have an indirect implication on the reliability of year-round supply of biomass to the biorefinery. Size reduction reduces the storage volume requirement. Moreover, densification such as pelletization also stabilizes biomass to a certain extent. This can allow storage of biomass beyond one year, and therefore provide a buffer against unexpected supply disturbances. Similarly, having more biomass at a central storage facility, as in the second scenario, will lead to more reliable supply since more efficient transport arrangements can be made to minimize the influence of disturbances. However, these aspects are not directly quantified in this study.

Sensitivity analysis

The experimental data along with the equipment data were adapted to develop relevant scenarios for our analysis. Therefore, we conducted a sensitivity analysis with respect to various attributes of the hammer mill to quantify their impact on the total cost and optimal particle size. The parameters considered were throughput of the hammer mill, cost of the hammer mill, and output bulk density of the biomass ground in a hammer mill. Since the impact of higher throughput on the other attributes of the hammer mill was not known, we assumed that the hammer mill

attributes such as cost, efficiency, and power requirement did not change with the throughput. In addition, we also conducted a sensitivity analysis with respect to the storage cost of ground biomass. The storage cost calculated by the model included the cost of building the infrastructure (Table S12 from supporting information) and the land cost. For on-farm storage, the cash rent value of \$0.0395 m^{-2} (\$160 per acre) for Illinois was used.[27] In contrast, land was assumed to be purchased to build a centralized storage facility, and hence the land value of \$1.1 m^{-2} for Illinois was used.[27] We assumed that the storage cost could be reduced by purchasing less expensive land or cost-efficient structures.

Additional scenarios for coarse size reduction to particle sizes of 12.7–25.4 mm and roll press compaction at farm gate have been studied in literature,[28–30] and may be considered as part of the future work.

Results and discussion

This section presents the important results of this work. The results of the size reduction and densification experiments are first presented followed by a discussion of how the results were adapted for model simulations. The simulation results are then presented in detail.

Size reduction and densification experiments

The results of size reduction experiments for Miscanthus showed that both bulk density and specific energy decreased according to a power law with increasing particle size (Fig. 5). The data were fitted to a power law regression curve using Microsoft Excel®, which was then used to determine the bulk density and energy consumption for the particle sizes of 16 mm and 25.4 mm. The results for switchgrass were similar to those for Miscanthus and are reported in the supporting information (Fig. S2).

The experimental data for densification of Miscanthus showed that bulk density was inversely proportional to the particle size while specific energy of densification was proportional to the particle size (Fig. 6). The data were fitted with a regression equation in the form of a power law using Microsoft Excel®, and the regression based values were used in model simulations. The regression curves were also used to determine values for 16 mm and 25.4 mm particle sizes via extrapolation. The results for switchgrass were similar to those for Miscanthus and are reported in the supporting information (Fig. S3).

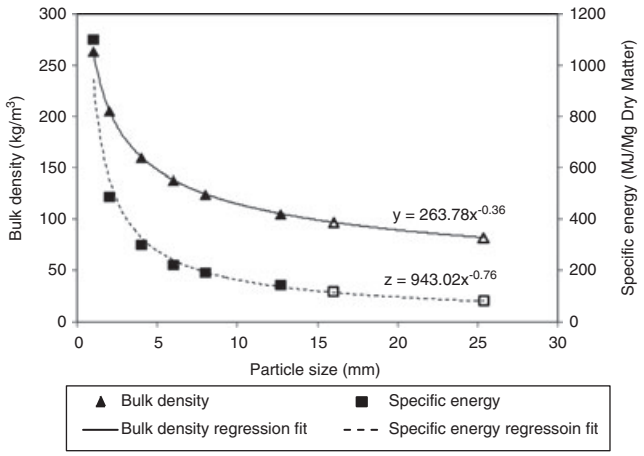

Figure 5. Variation in bulk density and specific energy consumption of size reduction with output particle size for Miscanthus along with their respective power law regression fits; In the regression equations x is particle size in mm, y is bulk density in kg/m^3 and z is specific energy in MJ/Mg dry matter; filled markers show values obtained by experiments while empty markers show regression estimates; similar trends were observed for switchgrass.

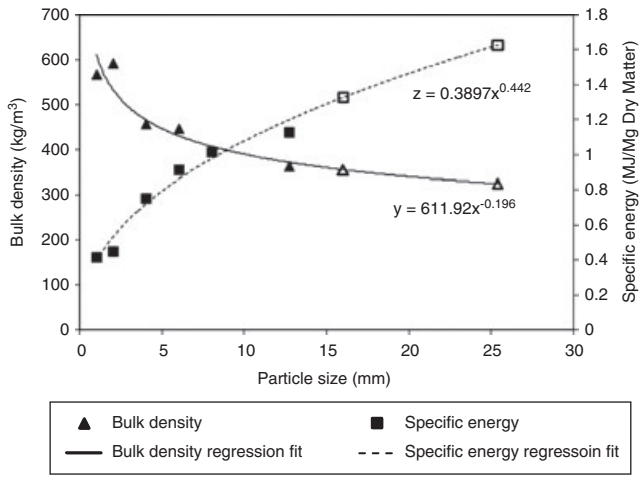

Figure 6. Variation in bulk density and specific energy of densification with particle size after densification by 1.2 MPa for Miscanthus along with their respective power law regression fits; In the regression equations x is particle size in mm, y is bulk density in kg/m^3 and z is specific energy in MJ/Mg dry matter; filled markers show values obtained by experiments while empty markers show regression estimates; similar trends were observed for switchgrass.

Details of size reduction and densification experiments and results have been reported by Miao *et al.*[6,11] The power laws between specific energy consumption and particle size and between bulk density of output particle and

particle size were also reported by Lam *et al*.[31] and Mani *et al*.,[32,33] respectively.

Data processing and adaptation

The size reduction experimental data for a particle size of 8 mm and lower were generated using a two-stage (coarse and fine) reduction with a hammer and knife mill. The two-stage size reduction regime was used in the laboratory because it is commonly used in the industry for material size reduction. Moreover, a hammer mill that could achieve particle sizes of interest while starting with fairly long stems of Miscanthus and switchgrass was not available. Ideally, the model should, therefore, also use the equipment performance data such as fixed and operating costs, energy consumption, and throughput for hammer and knife mill together. However, model relevant data were available only for the hammer mill, which was capable of achieving the particle sizes considered in this analysis. These data are shown in supporting information (Tables S4 and S8). Moreover, single equipment achieving the desired particle size would be preferred from a commercial production standpoint. Therefore, the model simulations assumed that the size reduction to all particle sizes was performed in a single stage with a hammer mill. The bulk density and specific energy consumption data from the experiments were assumed to be applicable for single stage hammer milling.

The throughputs for the hammer mill were also needed for the simulations. We assumed that the throughput for the knife mill used for the experiments and the hammer mill considered in the model were similar for 2 mm output particle size (4.53 Mg h^{-1}). The total measured specific energy consumption for experimental coarse and fine size reduction of Miscanthus to 2 mm was 490.7 MJ Mg^{-1}. By assuming that the efficiency of a commercial hammer mill was same as that of our experimental set-up, the total power requirement for the hammer mill was calculated as 617.5 kW. This would remain constant irrespective of the desired particle size since only the screen would be changed to achieve a specific particle size. Milling would take longer to achieve a smaller particle size, which will reduce the throughput and increase the specific energy consumption. Since the specific energy consumption for all particle sizes was known from experiments, those values along with the power of the hammer mill were used to calculate the throughputs. It was observed that the rates decreased almost linearly with particle size, which confirmed the experimental observations. Since the same hammer and knife mills were used to process switchgrass, the power requirement would be 617.5 kW. This value, along with the specific energy consumption obtained from switchgrass grinding experiments, was used to determine the throughput rates for switchgrass grinding. The throughputs for Miscanthus and switchgrass are reported in supporting information (Tables S4 and S8, and Fig. S4).

Base case scenario: Size reduction

The simulation results for the base case scenarios for Miscanthus (Fig. 7) indicated that the optimal particle size range was 4–6 mm. The cost for 4 mm was \$54.87 Mg^{-1} and that for 6 mm was \$54.65 Mg^{-1}, the difference being within the numerical tolerance to ascertain the true optimal size. For particle sizes smaller than 4 mm, the cost of grinding increased considerably and nonlinearly because the throughput of the hammer mill slowed significantly to achieve the smaller particle sizes. This increased the total cost even though the storage and transportation costs were low (Fig. 7). In contrast, for particle sizes larger than 6 mm, the grinding costs were low but the storage and transportation costs increased due to reduced bulk densities, which increased the total cost.

The results for the base case scenario for switchgrass production (Fig. 8) were qualitatively very similar to those for Miscanthus. The optimal particle size was 6 mm with the cost of \$60.77 Mg^{-1}, while the cost for 4 mm of \$61.53 Mg^{-1} was also very close to the optimal. The total cost of switchgrass production was slightly higher than that for Miscanthus for all particle sizes. The relatively small difference in cost despite the yield of Miscanthus being almost twice that of switchgrass was due to the way the scenarios were designed. The scenarios considered a

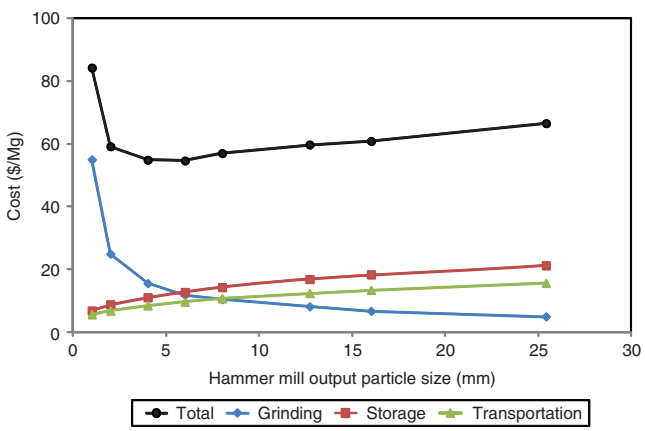

Figure 7. Variation of different costs of Miscanthus production and provision as a function of hammer mill output particle size.

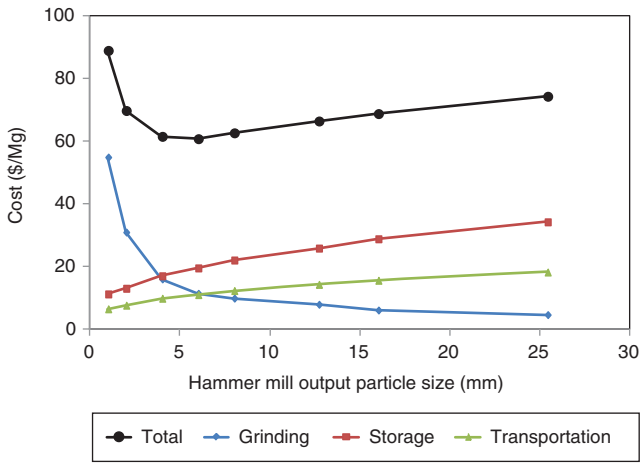

Figure 8. Variation in different costs for the production of switchgrass as a function of different hammer mill output particle sizes.

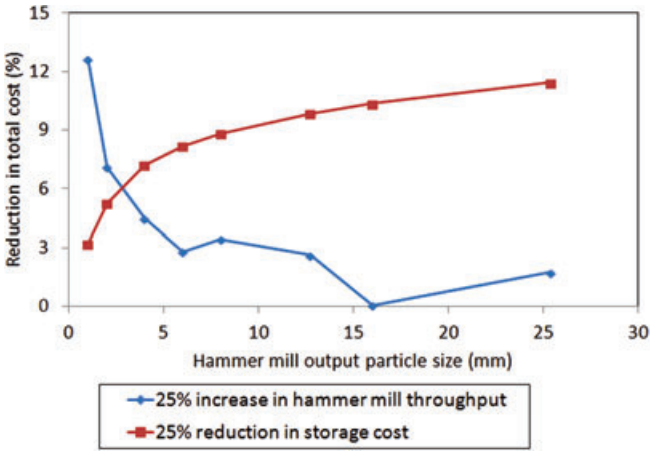

Figure 9. Sensitivity analysis – Impact of 25% higher throughput of the hammer mill and 25% lower storage cost on total cost of Miscanthus production for different particle sizes.

fixed collection area and the biorefinery capacities were optimized. Consequently, the optimal biorefinery capacity using Miscanthus feedstock for all particle sizes was about 2800 Mg d^{-1}, while that using switchgrass feedstock was about 1600 Mg d^{-1}. If the scenarios had been designed such that the biorefinery capacity was fixed, the cost of Miscanthus supply would have been much lower since the collection area would have been about 50% of that for switchgrass. In addition, hammer mill throughputs were lower for Miscanthus as compared to switchgrass, thereby impacting the relative costs (Tables S4 and S8 and Fig. S4 from supporting information).

The optimal equipment selection for each farm cannot be reported here. Apart from the grinder that was fixed for each scenario, all farms selected 'Mower' for harvesting Miscanthus and 'Mower conditioner' for harvesting switchgrass. For both feedstocks, 'Wheel Loader Bucket' was selected for loading, and 'Forage Wagon' was selected for in-field transport. The equipment number depended primarily on the farm size. Long-distance transportation of ground biomass was done using 'Bulk Trailer'.

Sensitivity analysis

Hammer mill throughput was incremented in the simulation by 25%, 50%, and 75% for each particle size and the percentage cost reduction was determined (Fig. 9 for 25% increase). Results showed that higher throughput reduced the total costs for smaller particle sizes substantially. However, its impact on the total cost of larger particle sizes was negligible. The percentage cost reduction for particle sizes of 6 mm and 16 mm did not follow this trend (Fig. 9). This was due to the approximate numerical approach of DDC used to solve BioFeed, which can converge to sub-optimal solutions within ±5% of the optimal solution.[17] The total cost, though, followed the expected trend and these plots are reported in the supporting information (Fig. S5). Importantly, 25% and 50% increase in throughput did not change the optimal particle size, and 75% increase in throughput made the optimal size to be 2–4 mm. The optimal costs for 25%, 50%, and 75% increase in hammer mill throughput were \$52.41 Mg^{-1}, \$50.52 Mg^{-1}, and \$49.43 Mg^{-1}, respectively. This implies that the hammer mill throughput had little impact on the optimal particle size range. Higher throughput also reduced the total energy consumption since the hammer mill needed to be operated for a shorter time, and this reduction was again higher for smaller particle sizes. However, this conclusion was subject to the assumption that the power consumption of the hammer mill remained constant at 617.5 kW.

The storage costs were reduced by 25%, 50%, and 75% for all storage options in the model (on-farm covered and satellite storage) for the sensitivity analysis. Figure 9 plots the percentage reduction in total cost for all particle sizes with respect to the base case values for corresponding particle sizes for 25% reduction in storage costs. Complete cost plots are reported in the supporting information (Fig. S6). Results showed that lower storage cost led to a substantial cost reduction for larger particle sizes while its impact on smaller particle sizes was negligible. However, the optimal particle size continued to be 6 mm. Cost reductions for 25.4 mm particle size were 11%, 23% and 34% for 25%,

50%, and 75% reduction in storage costs, respectively. The optimal costs for 25%, 50% and 75% reduction in storage costs were \$50.17 Mg^{-1}, \$45.70 Mg^{-1}, and \$41.23 Mg^{-1}, respectively. It should be emphasized that for the particle size of 4–6 mm, which was optimal for all scenarios, the impact of storage cost reduction was higher than that of hammer mill throughput increase. This could be used as a guide to focus technology improvement efforts.

The sensitivity analysis with respect to the grinding cost (fixed and operating) showed trends similar to those for hammer mill throughput and are reported in the supporting information (Figs S7 and S8). The cost of grinding was significantly higher for smaller particle sizes. Hence, any reduction in grinding cost, possibly due to better equipment, led to significant reduction in total cost. The results for the sensitivity analysis with respect to the output bulk density of the hammer mill are discussed in the supporting information (Fig. S9).

Similar sensitivity analyses were also conducted for switchgrass production. The results were qualitatively similar to those observed for Miscanthus and hence not discussed here. The results are reported in the supporting information (Figs S10–S15).

Impact of angle of repose

The model assumed that on-farm storage sheds with three walls will have 10% buffer for safety and operational flexibility. However, 90% utilization of available storage volume may not be possible since ground biomass must be piled in a heap leaving a significant volume unused. The fraction of this unused volume will depend on the angle of repose of ground biomass. The angle of repose of a granular material is the steepest angle of descent or dip of the slope relative to the horizontal plane when material on the slope face is on the verge of sliding. Preliminary experiments showed that the angle of repose of ground Miscanthus was about 45°. Assuming that biomass can be piled up against one wall of the shed up to its roof, a 45° angle of repose implies that only 50% volume of the shed can be utilized. Total costs for different particle sizes with this assumption were calculated and compared with the base case costs (Fig. 10). As expected, costs increased substantially for larger particle sizes due to the greater storage volume requirement. The optimal particle size after the angle of repose consideration reduced to about 2–4 mm. The cost for 2 mm was \$67.67 Mg^{-1} and that for 4 mm was \$67.68 Mg^{-1}, the difference being within the numerical tolerance to ascertain the true optimal size.

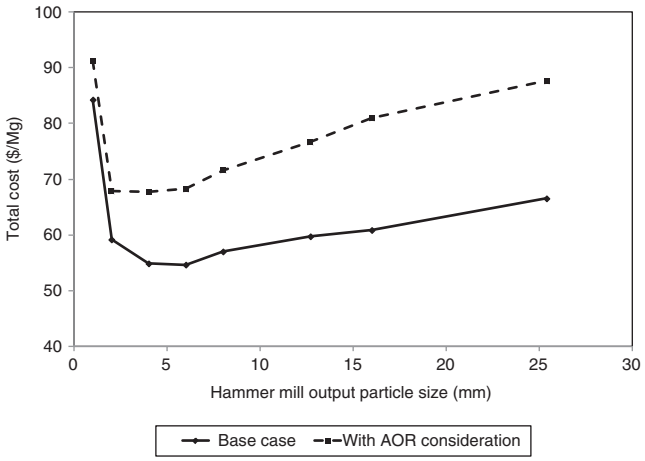

Figure 10. Impact of the consideration of angle of repose (AOR) of ground biomass on the total cost of Miscanthus production and its comparison with base case.

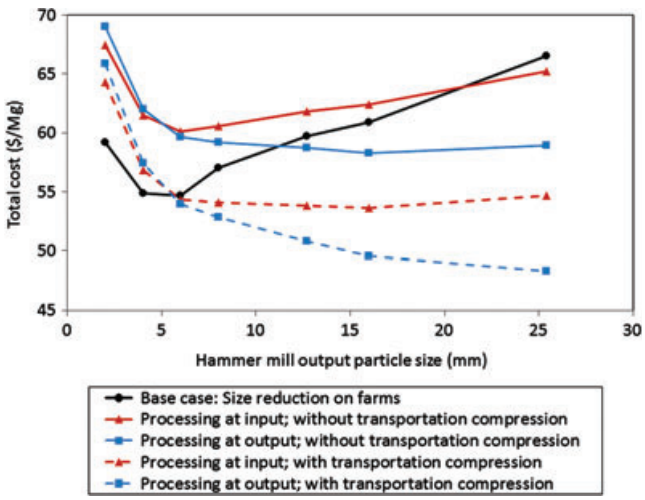

Figure 11. Miscanthus production cost for scenarios with centralized storage and pre-processing (CSP) with and without densification during transportation and its comparison with base case.

Size reduction and densification scenario for Miscanthus

As described previously, four scenarios were modeled after incorporating CSPs with size reduction and possible densification. Figure 11 compares the total cost of Miscanthus production for all four possibilities with the base case scenario previously discussed. The costs for 1 mm particle size are not shown in Fig. 11 since those costs were much higher in all cases and therefore could be ignored.

The cost trends are a function of the relative costs of size reduction, storage and transportation. Two points that need to be highlighted before discussing the results are:

- For the base case, only one pre-processing step of size reduction was performed. In contrast, the scenarios with CSPs necessitated two pre-processing steps, namely, baling at the farms and size reduction at the CSPs. Miscanthus baling was quite expensive since the hay equipment was not efficient and dedicated equipment is not yet available. The average cost of Miscanthus baling was about \$21 Mg^{-1}. In the size reduction and densification scenarios, farms performed baling while grinding was performed at the CSPs. The total cost of pre-processing for the scenarios with CSPs, therefore, was significantly higher for particle sizes of 4 mm and higher (Fig. S20 in supporting information).
- The storage and transportation costs depend on the bulk density of the feedstock. Here, it is important to note that for particle sizes of 4 mm and smaller, the bulk density of ground biomass was higher than the bale density (150 kg m^{-3}), while it was lower than the bale density for other particle sizes. Therefore, storage and transportation of baled biomass became more economical than ground biomass when particle size was greater than 4 mm. Since the density of the feedstock at the time of transportation and storage changes for different scenarios, the costs also change accordingly (Figs S21 and S22 in supporting information).

The total costs shown in Fig. 11 were the result of the interplay between the relative costs of storage and transportation with respect to the pre-processing costs.

Without any transportation compression, when pre-processing was performed at the input of the CSPs, the optimal particle size was 6-8 mm, the costs being \$60.10 Mg^{-1} for 6 mm and \$60.55 Mg^{-1} for 8 mm. The relative cost trends provided important insights. The total cost for this scenario was higher than that for the base case for all particle sizes except 25.4 mm. At particle sizes of 16 mm and lower, the higher cost of performing two pre-processing steps dominated the total cost. The difference started to reduce for particle sizes of 6 mm and higher because biomass of density lower than the bale density was being handled all along the supply chain in the base case. In contrast, when CSPs were used, the on-farm storage and first leg of transport was of biomass of higher density (bale density). This difference eventually became so high that the total cost for the CSP scenario was lower for the particle size of 25.4 mm.

When pre-processing was performed at the output of the CSPs, two important changes were observed:

1. The optimal particle size was 16 mm and the optimal total cost was \$58.29 Mg^{-1}. The costs for 12.7 mm and 25.4 mm where within ±\$1 Mg^{-1} of the optimal cost. In this scenario, biomass was stored in the CSPs in baled form, which meant that the cost of storage for the scenario did not increase with the particle size (Fig. S21 in supporting information). Only the transportation cost between CSPs and the biorefinery was increasing with particle size (Fig. S22 in supporting information). Therefore, the optimal particle size was much larger than that for the base case. For the particle size of 25.4 mm, the transportation cost between CSPs and the biorefinery increased substantially to render that size sub-optimal.
2. The particle size at which the costs curves for base case and the CSP scenario intersected each other was between 8 mm and 12.7 mm, which was much lower as compared to that for the scenario with pre-processing at the input of the CSPs. The reason again was the independence of storage cost with particle size. When pre-processing was performed at the input of CSPs, the storage cost increased with particle size. In contrast, the storage cost remained constant when pre-processing was at the output. Therefore, as particle size increased, the benefit of having CSPs at the output became stronger since greater savings in storage were observed. This led to the cost of the scenario becoming lower than that for the base case at a much smaller particle size.

The comparison also showed that the optimal total cost was the lowest for the base case scenario among these three scenarios (\$54.65 Mg^{-1}). This suggested that installing CSPs without transportation densification capability was not advisable. It may provide other benefits such as lower influence of supply disturbance as mentioned earlier. Moreover, biomass quality preservation may be better, which was not modeled here.

Figure 11 also shows the plots for the scenarios when the transportation between CSPs and biorefinery was performed in a densified form. We have again compared the options of pre-processing Miscanthus at the input or the output of the CSPs. The optimal particle size for pre-processing at the input of CSPs was 16 mm, and the optimal cost was \$53.62 Mg^{-1}. However, the costs for particle sizes from 6 mm to 25.4 mm were within ±\$1 Mg^{-1} of the optimal cost, indicating that the identification of a unique optimum was not possible. The optimal particle size when

pre-processing was at the output of the CSPs was 25.4 mm and the optimal cost was \$48.31 Mg^{-1}. The results showed that the benefit of pre-processing at the output instead of the input was also observed in these scenarios.

An important observation when compared to the CSP scenarios without densification was that the total costs were much lower, and that was true for both possibilities of conducting pre-processing at the CSPs. This was expected since densification made transportation of ground biomass much less expensive (Fig. S22 in supporting information). Another important difference was that the cross-over points for the costs with the base case for both scenarios were around the particle size of 6 mm. This was because densification during transportation reduced the high transportation costs associated with larger particle sizes. Therefore, such a system could take advantage of the fact that size reduction to larger particle sizes was less expensive and transportation was also less expensive due to densification. This made the scenarios more economical at lower particle sizes. Consequently, the optimal particle sizes for both these scenarios were much larger.

Contrary to scenarios without any densification, the optimal costs for both scenarios with densification were lower than the optimal costs for the base case. While the difference for scenario with pre-processing at CSP input was small (\$1.03 Mg^{-1}), the difference for the scenario with pre-processing at CSP output was \$6.31 Mg^{-1}. As mentioned earlier, the model did not consider the cost of densification through compression. Therefore, the cost savings need to be properly interpreted. The cost difference represents the upper bound on the total investment to set up and operate the infrastructure for biomass densification. We need to calculate the total capital and operating cost of the biomass densification equipment at CSPs and specialized trucks needed to transport the densified biomass. If this cost on a per unit biomass basis is less than \$6.31 Mg^{-1}, then it is beneficial to set-up such a supply system. The quantification of this upper bound is an important result of this work.

The optimal equipment selection for each farm cannot be reported here. All farms selected 'Mower' for harvesting and 'Baler (contractor)' for baling. 'Gooseneck Trailer' was used for bale transport within the farm, and the 'Telescopic Bale Loader' was used for loading onto the transportation truck. The equipment number depended primarily on the farm size. Long distance transportation of baled biomass was done using 'F-40 Flatbed Trailer', while that of ground biomass was done using 'Bulk Trailer'.

Size reduction and densification scenario for switchgrass

The same scenarios with the consideration of CSPs as modeled for Miscanthus were also modeled for switchgrass. The total cost was again a function of the relative pre-processing, storage, and transportation costs as a function of different particle sizes. The independent cost curves for these categories have been reported in the supporting information (Figs S24–S27). Figure 12 shows the total cost curves for the four scenarios and compares those with the base case cost curve for switchgrass.

Compared to the results for Miscanthus, an important difference for switchgrass was that the costs of all scenarios with CSPs were lower than that for the base case scenario for all particle sizes. Thus, the crossover of the cost curves was not observed. This was mainly due to the significantly lower baling cost for switchgrass. Baling was much cheaper for switchgrass than Miscanthus since hay baling equipment could be used. The average cost of baling was about \$11.2 Mg^{-1}. Baling was also significantly less expensive than grinding for switchgrass, while the two costs for Miscanthus were comparable. Moreover, grinding of switchgrass at CSPs was cost-effective since a large amount was being processed, thereby taking advantage of the economy of scale. Therefore, when the CSPs were installed, the farms could bale biomass, which reduced the total on-farm production cost. The total pre-processing cost for the system did not increase much as compared to Miscanthus. The

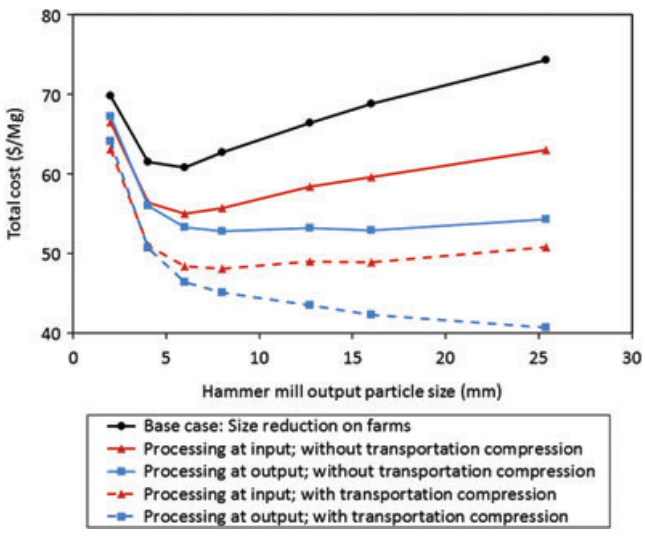

Figure 12. Switchgrass production cost for scenarios with centralized storage and pre-processing (CSP) with and without densification during transportation and its comparison with base case.

Table 1. The optimal particle size and cost of all scenarios modeled in this work for Miscanthus and switchgrass; the difference between the optimal costs for scenarios with size reduction at CSPs as compared to the base case scenario.

	Miscanthus			Switchgrass		
	Optimal size (mm)	Optimal cost ($ Mg^{-1})	Reduction from base case ($ Mg^{-1})	Optimal size (mm)	Optimal cost ($ Mg^{-1})	Reduction from base case ($ Mg^{-1})
Base case: Size reduction at farms	6	54.65	–	6	60.77	–
Size reduction at CSP input; no densification	6	60.10	–5.54	6	55.0	5.77
Size reduction at CSP output; no densification	16	58.29	–3.64	8	52.73	8.04
Size reduction at CSP input; densification for transportation	16	53.62	1.03	8	48.12	12.65
Size reduction at CSP output; densification for transportation	25.4	48.31	6.34	25.4	40.64	20.13

storage cost for the CSP scenario reduced since baled biomass required less expensive on-farm storage options than ground biomass. The overall effect was that the total cost of production was lower for the scenario with pre-processing at the CSPs. As the ground biomass particle size increased beyond 4 mm, the scenario with CSPs became even more attractive since baled biomass of higher density was being handled in the first storage and transportation operations while the loose ground biomass needed to be handled only between CSPs and biorefinery. These differences in results for Miscanthus and switchgrass emphasized the complex interaction among different stages of feedstock production and provision, which could be different for different energy crops. This highlights the value of a system-level model like BioFeed to provide case specific recommendations.

With pre-processing at the input of the CSPs and no densification, the optimal particle size was 6–8 mm with a cost of \$55 Mg^{-1} for 6 mm and \$55.7 Mg^{-1} for 8 mm. This was a reduction of \$5.77 Mg^{-1} from the base case. When pre-processing was performed at the output of the CSPs without densification, the costs reduced for a particle size of 6 mm and higher, and this reduction was higher for larger particle sizes. This observation was similar to that for Miscanthus and the reason has been explained in the previous section. The optimal particle size was 8 mm with the cost of \$52.73 Mg^{-1}. However, the costs for 6, 12.7, and 16 mm particle sizes were within ±\$1 Mg^{-1} of the optimal cost, indicating that the identification of a unique optimum was not possible. The optimal cost was \$8.04 Mg^{-1} lower than the optimal cost for the base case. These results indicated that the installation of CSPs provided definite benefits when size reduction was to be performed.

The addition of densification to size reduction further reduced the total cost for scenarios with processing at the input as well as the output of the CSPs. As explained previously, this was due to the reduced cost of transportation of switchgrass between the CSPs and the biorefinery, and this effect was magnified for larger particle sizes. The optimal particle size with pre-processing at the input was 8 mm. The optimal cost was \$48.12 Mg^{-1}, but the costs for 6, 12.7, and 16 mm particle sizes were within ±\$1 Mg^{-1} of the optimal cost. The reduction in the optimal cost as compared to that for the base case was \$12.65 Mg^{-1}. The optimal particle size with pre-processing at the output was 25.4 mm with the cost of \$40.64 Mg^{-1}, a reduction of \$20.13 Mg^{-1} over the optimal cost for the base case. As mentioned previously, these differences provide upper bounds on the investment into the necessary equipment since those costs have not been included in the cost calculations.

The optimal equipment selection for each farm cannot be reported here. All farms selected 'Mower conditioner' for harvesting. The smaller farms selected a 'Round Baler' while the larger farms selected a 'Square Baler'. 'Gooseneck Trailer' was used for bale transport within the farm, and the 'Telescopic Bale Loader' was used for loading onto the transportation truck. The equipment number depended primarily on the farm size. Long distance transportation of baled biomass was done using 'F-40 Flatbed Trailer', while that of ground biomass was done using 'Bulk Trailer'.

Table 1 summarizes the optimal particle size and cost values for all the scenarios for both crops studied in this work.

Conclusions

The determination of the optimal particle size and densification level of biomass feedstock is very important: It is a trade-off between the cost of size reduction (grinding)

and densification through compression and the efficiency in storage, transportation, as well as conversion. This work integrated experimental and modeling work to provide quantitative insights on this topic. Grinding and densification data for Miscanthus and switchgrass generated using experiments were incorporated in BioFeed, a system-level optimization model, to simulate different supply chain configurations. The results showed that 4–6 mm was the optimal particle size for both Miscanthus and switchgrass. The optimal costs were \$54.65 Mg^{-1} for Miscanthus and \$60.77 Mg^{-1} for switchgrass. Sensitivity analysis showed that although the hammer mill throughput, cost, and output bulk density impacted the total cost for all particle sizes, significant changes from the base case values were needed to lead to a different optimal particle size. Since densification at farms was not expected to be practical, scenarios with size reduction and densification at the county specific centralized storage and pre-processing facilities were simulated. Results showed that such a system could reduce the total costs by as much as \$6.34 Mg^{-1} for Miscanthus and \$20.13 Mg^{-1} for switchgrass over the base case. However, cost of achieving such densification must be considered to determine the real cost reduction. Therefore, the cost differences provided the upper bound on the investments that could be made to set-up and operate such systems. In the future, a similar analysis must be conducted for biomass processing so that the optimal particle size from the whole systems perspective can be determined.

Acknowledgement

This work has been funded by the Energy Biosciences Institute through the program titled 'Engineering Solutions for Biomass Feedstock Production'.

References

1. Perlack RD, Wright LL, Turhollow AF, Graham RL, Stokes BJ and Erbach DC, *Biomass as feedstock for bioenergy and bioproducts industry: The technical feasibility of a billion-ton annual supply,* DOE/GO-102005-2135, ORNL/TM-2005/66. Oak Ridge National Laboratory, Oak Ridge, TN (2005).
2. Somerville C, The billion-ton biofuels vision. *Science* **312**:1277 (2006).
3. Richard TL, Challenges in scaling up biofuels infrastructure. *Science* **329**:793–796 (2010).
4. Tumuluru JS, Wright CT, Hess JR and Kenney KL, A review of biomass densification systems to develop uniform feedstock commodities for bioenergy application. *Biofuel Bioprod Bioref* **5**:683–707 (2011).
5. Hess JR, Wright CT, Kenney KL and Searcy E, *Uniform-format solid feedstock supply system: A commodity-scale design to produce an infrastructure-compatible bulk solid from lignocellulosic biomass*, INL/EXT-09-15423. Idaho National Laboratory, US Department of Energy, Washington DC (2009).
6. Miao Z, Grift TE, Hansen AC and Ting KC, Energy requirement for comminution of biomass in relation to particle physical properties. *Ind Crop Prod* **33**:504–513 (2011).
7. Khullar E, Dien BS, Rausch KD, Tumbleson ME and Singh V, Effect of particle size on enzymatic hydrolysis of pretreated Miscanthus. *Ind Crop Prod* **44**:11–17 (2013).
8. Shastri YN, Hansen AC, Rodriguez LF and Ting KC, Development and application of BioFeed model for optimization of herbaceous biomass feedstock production. *Biomass Bioenerg* **35**:2961–2974 (2011).
9. Shastri YN, Hansen AC, Rodriguez LF and Ting KC, Optimization of Miscanthus harvesting and handling as an energy crop: BioFeed model application. *Biol Eng Trans* **3**:37–69 (2010).
10. ASABE, *Cubes, pellets, and crumbles—definitions and methods for determining density, durability, and moisture content,* ASAE S269.4, DEC1991 (R2007). American Society of Agricultural and Biological Engineers, St Joseph, MI (2007).
11. Miao Z, Grift TE, Hansen AC and Ting KC, Energy requirement for lignocellulosic feedstock densifications in relation to particle physical properties, pre-heating and binding agents. *Energy Fuels* **27**:588–595 (2013).
12. Han JK, Collins M, Newman MC and Dougherty CT, Effects of forage length and bale chamber pressure on pearl millet silage. *Crop Sci* **46**:337–344 (2006).
13. Shastri YN, Hansen AC, Rodriguez LF and Ting KC, Advances in systems informatics and analysis of biomass feedstock production for bioenergy. *Pertanika J Sci Technol* **21**:273–280 (2013).
14. Shastri YN, Rodriguez LF, Hansen AC and Ting KC, Impact of distributed storage and pre-processing on Miscanthus production and provision systems. *Biofuel Bioprod Bioref* **6**:21–31 (2012).
15. Shastri YN, Hansen AC, Rodriguez LF and Ting KC, Impact of probability of working day on planning and operation of biomass feedstock production systems. *Biofuel Bioprod Bioref* **6**:281–291 (2012).
16. Rosenthal RE, *GAMS - A User's Guide.* GAMS Development Corporation, Washington, DC (2008).
17. Shastri YN, Hansen AC, Rodriguez LF and Ting KC, A novel decomposition and distributed computing approach for the solution of large scale optimization models. *Comput Electron Agric* **76**:69–79 (2011).
18. Vilsack T and Clark CZF, *2007 Census of Agriculture: United States Summary and State Data, volume 1, Geographic Area Series, Part 51,* AC-07-A-51. United States Department of Agriculture, Washington DC (2007).
19. Heaton E, Voigt T and Long S, A quantitative review of comparing the yields of two candidate C4 biomass crops. *Biomass Bioenerg* **27**:21–30 (2004).
20. Smeets EMW, Lewandowski IM and Faaij APC, The economical and environmental performance of miscanthus and switchgrass production and supply chains in a European setting. *Renew Sust Energ Rev* **13**:1230–1245 (2009).
21. Venturi P, Huisman W and Molenaar J, Mechanization and costs of primary production chains for Miscanthus x Giganteus in The Netherlands. *J Agr Eng Res* **69**:209–215 (1998).
22. ASABE, *Agricultural Machinery Management Data,* ASAE D497.5 MAR2011. American Society of Agricultural and Biological Engineers, St. Joseph, Michigan (2011).
23. ASABE, *Agricultural Machinery Management,* ASAE EP496.3 FEB2006. American Society of Agricultural and Biological Engineers, St Joseph, MI (2006).

24. Kumar A, Sokhansanj S, Switchgrass (Panicum vigratum, L) delivery to a biorefinery using integrated biomass supply analysis and logistics (IBSAL) model. *Bioresource Technol* **98**:1033–1044 (2007).
25. Sokhansanj S, *Feedstock Collection and Logistics: Reduce Costs, Optimize Resources*. ASABE, St. Joseph, MI (2009).
26. Eranki PL, Bals BD and Dale BE, Advanced regional biomass processing depots: A key to the logistical challenges of the cellulosic biofuel industry. *Biofuel Bioprod Bioref* **5**:621–630 (2011).
27. USDA, *Land Values and Cash Rents 2008 Summary.* United States Department of Agriculture, National Agricultural Statistics Services, Washington DC (2008).
28. Morey RV, Kaliyan N, Tiffany DG and Schmidt DR, A corn stover supply logistics system. *Appl Eng Agric* **26**:455–461 (2010).
29. Kaliyan N, Schmidt DR, Morey RV and Tiffany DG, Commercial scale tub grinding of corn stover and perennial grasses. *Appl Eng Agric* **28**:79–85 (2012).
30. Kaliyan N, Morey RV and Schmidt DR, Roll press compaction of corn stover and perennial grasses to increase bulk density. *Biomass Bioenerg* **55**:322–330 (2013).
31. Lam PS, Sokhansanj S, Bi X, Lim CJ, Naimi LJ, Hoque M *et al.,* Bulk density of wet and dry wheat straw and switchgrass particles. *Appl Eng Agric* **24**:351–358 (2008).
32. Mani S, Tabil LG and Sokhansanj S, Grinding performance and physical properties of wheat and barley straws, corn stover and switchgrass. *Biomass Bioenerg* **27**:339–352 (2004).
33. Mani S, Tabil LG and Sokhansanj S, Effects of compressive force, particle size and moisture content on mechanical properties of biomass pellets from grasses. *Biomass Bioenerg* **30**:648–654 (2006).

Yogendra Shastri

Yogendra Shastri is an assistant professor in the Department of Chemical Engineering at IIT Bombay, India. He has a PhD from the University of Illinois and has worked at EBI as a research assistant professor. He specializes in developing and applying systems-theory-based approaches to bioenergy, environment, and sustainability.

Zewei Miao

Zewei Miao is a research assistant professor in biomass feedstock preprocessing and transportation at the Energy Biosciences Institute, University of Illinois. He has worked on ecological and environmental modeling at the Chinese Academy of Sciences, the Catholic University of Italy, the Canadian Forest Services, McGill University, and Rutgers University.

Luis Rodriguez

Luis Rodriguez is an associate professor at University of Illinois at Urbana-Champaign. He has an interdisciplinary PhD from Rutgers University and has worked as a postdoctoral fellow at the NASA Johnson Space Center. He specializes in the modeling, simulation, and analysis of biological systems.

Tony E. Grift

Tony E. Grift is an associate professor in the Department of Agricultural and Biological Engineering, University of Illinois. As a principal investigator, he is leading the Biomass Transportation Task within a program titled 'Engineering Solutions for Biomass Feedstock Production', which is part of the BP-funded Energy Biosciences Institute.

Alan C. Hansen

Alan C. Hansen is a professor in the Department of Agricultural and Biological Engineering, University of Illinois. He has been the leader for biomass harvesting research in a BP-funded Energy Biosciences Institute program. His research interests include biofuels, biomass feedstock production, and agricultural machinery systems.

K.C. Ting

K.C. Ting, PhD, is Professor and Head of the Agricultural and Biological Engineering Department, University of Illinois. He specializes in agricultural systems informatics and analysis. He currently leads a BP Energy Biosciences Institute program on 'Engineering Solutions for Biomass Feedstock Production'. He is Fellow of ASABE and ASME.

